

## ANALYSIS OF MULTILAYERED COMPOSITE PLATES BY LOCAL PETROV-GALERKIN METHOD

Daniel Riecky\*, Milan Žmindák\*\*, Martin Dudinský\*\*, Zoran Pelagić\*\*

*This paper focuses on the implementation of the MLPG formulation for layered plates. For this purpose implementation of homogenization theory was required and analyses were performed in order to obtain homogenized material properties of composite plates. Software for homogenization of material properties uses direct homogenization method that is based on volume average of stresses in the representative volume element (RVE). Homogenization is performed by linking MATLAB and ANSYS software. Obtained data are used in analyses carried out in own software which is based on the MLPG method. Strain, stress and displacement fields were evaluated. Results obtained by MLPG were compared with those obtained by FEM programs ANSYS and ABAQUS.*

*Keywords: composite plates, unidirectional composites, Reissner-Mindlin theory, meshless method*

### 1. Introduction

The finite element method (FEM) is one of the most widely used and most popular numerical methods for analyzing plate structures. Although the method is stable, well developed and has reached extensive development during last decades, it also has some limitations [1].

In last years an increase of interest in new type of numerical methods known as meshless methods was observed [2, 3]. These methods are interesting due to their flexibility and ability of solving boundary value problems without predefined mesh. One of the areas where meshless methods are convenient to use is analysis of plate and shell structures. These methods are useful due to flexibility of meshless algorithms and ability of meshless approximation functions to obtain interpolating field with high order of continuity in a simple way. In some cases it is possible to overcome some ‘locking’ effects in more simple way than in FEM. Meshless methods are relatively new concept in computational mechanics. Compared to FEM formulations there are less meshless formulations available for plate and shell structures. Additional research and development of general meshless methods able to successfully solve various problems in plate structural analyses is therefore necessary. Meshless approaches proved to be successful in modeling of functionally graded materials (FGM) [4, 5].

This paper also focuses on implementation of the MLPG formulation for layered plates. Strain, stress and displacement fields were evaluated. Results obtained by MLPG were compared with those obtained by FEM programs ANSYS and ABAQUS.

---

\* Ing. D. Riecky, PhD., Plastic Omnium Auto Exteriorx, Ltd., 900 55 Lozorno, Slovakia

\*\* prof. Ing. M. Žmindák, CSc., Ing. M. Dudinský, Ing. Z. Pelagić, University of Žilina, Faculty of Mechanical Engineering, Department of Applied Mechanics, Univerzitná 1, 010 26 Žilina, Slovak Republic

## 2. Homogenization of composite

### 2.1. Homogenization techniques

Some analytical and numerical techniques have been used for prediction and characterization of composite microstructure behaviour. Analytical methods provide reasonable prediction for relatively simple configurations of the phases. Complicated geometries, loading conditions and material properties often do not yield analytical solutions, due to complexity and number of equations. In this case, numerical methods are used for approximate solving, but they still make some simplifying assumptions about the microstructures of heterogeneous multiphase materials.

There are various homogenization methods. Direct homogenization is based on the volume average of field variables, such as stress, strain and energy density. Effective properties can be calculated from effective properties definitions. The average and calculation of field variables can be performed numerically, for example by FEM or boundary element method and geometry and microstructural properties can be generalized for real composite materials which do not have periodic structure distribution of the fibers in the matrix [6].

Indirect homogenization is based on the Eshelby solution of self-deformation for one inclusion in an infinite matrix – the equivalent inclusion method [7]. An alternative approach to direct and indirect homogenization is the variational method, which can determine the upper and lower limits of the elasticity modulus [8].

A relatively new approach for a homogenization of microstructures consists of mathematical homogenization based on a two-scale extension of the displacement field [9].

### 2.2. Results of homogenization

This part describes a procedure of homogenization of material properties of composites using the method of representative volume element (RVE). For the analysis of material properties an own software in MATLAB language was programmed and a part of the solution was carried out in ANSYS software. The RVE consists of volume elements and then it is loaded by unit strains in various directions. The effective lamina properties are obtained from the volume means of stress values obtained by loading of the RVE.

Homogenized lamina RVE consists of fibers and epoxy matrix. The fibers are from three material types: carbon, glass, polyaramid (kevlar). The RVE dimensions are calculated

	Fiber material		
	Carbon	Fiberglass	Kevlar
	M40J	S2Glass	K49
$E_f$ [GPa]	377	85.5	135.5
$F_{1t}$ [GPa]	4.41	4.6	3.5
$\nu$	0.33	0.22	0.37
$\rho_f$ [kg/m <sup>3</sup> ]	1770	2490	1450
$d_f$ [ $\mu$ m]	5	10	10

Tab.1: Fiber material properties

Matrix material	$E_m$ [GPa]	$F_{1t}$ [MPa]	$\nu$	$\rho_m$ [kg/m <sup>3</sup> ]	$G_m$ [GPa]
Epoxy	3.45	70	0.3	85.5	1.33

Tab.2: Matrix material properties

for the hexagonal fiber configuration and for the square configuration [10]. We assumed cylindrical fiber shapes and an ideal cohesion between the fiber and the matrix. Used carbon fibers have an industrial label T300 and M40J. The glass fiber label is EGlass and S2Glass. Polyaramide fibers have the label K49. Fiber material properties are listed in Table 1 and the matrix properties are listed in Table 2, where subscript 'f' denotes fiber and 'm' matrix, respectively and  $E$  – Young modulus,  $G$  – shear modulus,  $F_{1t}$  – longitudinal tensile strength,  $\nu$  – Poisson number,  $\rho$  – density,  $d_f$  – fiber diameter.

The RVE dimensions are calculated for the hexagonal fiber configuration Fig. 1a, from the relations

$$a_2 = \sqrt{\frac{1}{8} \frac{\pi d_f^2}{V_f \tan(60^\circ)}}, \quad a_3 = a_2 \tan(60^\circ), \quad a_1 = 0.5 a_2 \quad (1)$$

and for the square fiber configuration the RVE dimensions are in Fig. 1b, from the relations

$$a_2 = \sqrt{\frac{1}{8} \frac{\pi d_f^2}{V_f \tan(60^\circ)}}, \quad a_3 = a_2 \tan(60^\circ), \quad a_1 = 0.5 a_2 \quad (2)$$

where  $1$  is the  $x$  direction, in this case the fiber direction,  $2$  is the  $y$  direction, orthogonal to the fiber direction,  $3$  in direction  $z$ , transverse vertical to the fiber direction.

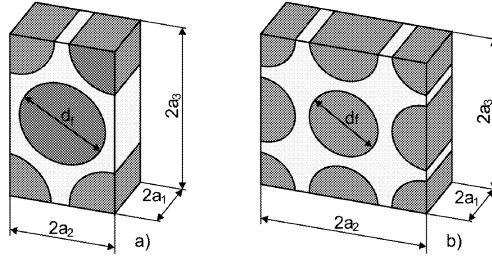


Fig.1: Representative volume elements, a) hexagonal configuration, b) square configuration

The four elastic properties of the homogenized material can be computed by [11]:

$$\begin{aligned} E_1 &= C_{11} - \frac{2 C_{12}^2}{C_{22} + C_{23}}, \\ \nu_{12} &= \frac{C_{12}^2}{C_{22} + C_{23}}, \\ E_2 &= \frac{(C_{11} (C_{22} + C_{23}) - 2 C_{12}^2) (C_{22} - C_{23})}{C_{11} C_{22} - C_{12}^2}, \\ G_{12} &= C_{66}. \end{aligned} \quad (3)$$

In order to evaluate the elastic matrix  $C$  of the composite, the RVE is subjected to an average strain. Then the volume average of the strain in the RVE equals to the applied strain

$$\bar{\varepsilon}_{ij} = \frac{1}{V} \int_V \varepsilon_{ij} dV \quad (4)$$

The components of the tensor  $\mathbf{C}$  are determined solving three elastic models of RVE with parameters  $(a_1, a_2, a_3)$  subjected to the boundary conditions (BC). The unit strain applied on the boundary results in a complex state of stress in the RVE. Then volume average of stress in RVE equals to required components of the elastic matrix as

$$C_{ij} = \bar{\sigma}_i = \frac{1}{V} \int_V \sigma_i dV . \quad (5)$$

The coefficients in  $\mathbf{C}$  are found by setting a different problem for each column of  $\mathbf{C}$  and the components are determined using three steps listed in [11]. Homogenization of composite plate is performed by linking MATLAB and ANSYS software and final results are given in Table 3, where the indices ‘h’ and ‘s’ denotes hexagonal array and square array, respectively.

$V_f = 0.6$	M40J		S2Glass		K49	
	h	s	h	s	h	s
$E_1$ [GPa]	227.58	227.58	52.683	52.687	82.683	82.685
$E_2$ [GPa]	12.831	16.71	11.607	14.334	12.121	15.301
$G_{12}$ [GPa]	5.15	5.53	4.67	4.94	4.844	5.155
$G_{23}$ [GPa]	4.737	6.967	4.3314	5.905	4.481	6.288
$\nu_{12}$	0.320	0.321	0.246	0.245	0.347	0.348
$\nu_{23}$	0.354	0.199	0.340	0.214	0.352	0.217

Tab.3: Material properties for composite with fiber volume fraction of  $V_f = 0.6$

### 3. Governing equations

The Mindlin-Reissner laminated theory of plates was formulated by deriving classical plate theory for composite plates. In this theory the plate composes of  $N$  orthotropic layers with total thickness  $h$ . The midsurface of layered plate is located in the region  $\Omega$ , in plane  $(x_1, x_2)$ . Axis  $x_3 \equiv z$  is perpendicular to the midsurface (Fig. 2).  $k$ -th layer is located between coordinates from  $z = z_k$  to  $z = z_{k+1}$  in thickness direction  $x_3$ .

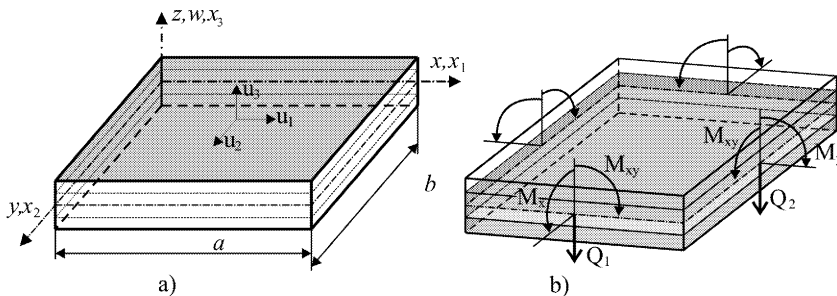


Fig.2: Composite plate a) geometry and displacements, b) moments and shear forces

If  $k$ -th lamina is from orthotropic material, then the relation between stresses  $\sigma_{ij}$  and strains  $\varepsilon_{mn}$  is expressed by the constitutive equation for stress tensor

$$\sigma_{ij}^{(k)}(\mathbf{x}, x_3, t) = c_{ijmn}^{(k)} \varepsilon_{mn}(\mathbf{x}, x_3, t) , \quad (6)$$

with assumption of homogeneous coefficients of the constitutive tensor  $c_{ijmn}^{(k)}$  for  $k$ -th lamina. In the case of layer-wise continuous material properties the following constitutive equations are obtained for bending moments  $M_{\alpha\beta}$  and shear forces  $Q_\alpha$ ,  $\alpha, \beta = 1, 2$  for orthotropic plate

$$\begin{aligned} M_{\alpha\beta} &= D_{\alpha\beta} (w_{\alpha,\beta} + w_{\beta,\alpha}) + C_{\alpha\beta} w_{\gamma,\gamma} , \\ Q_\alpha &= C_\alpha (w_\alpha + w_{3,\alpha}) . \end{aligned} \tag{7}$$

We note that for repeated indices  $\alpha$  and  $\beta$  in (7) Einstein summation rule does not apply and material parameters  $D_{\alpha\beta}$ ,  $C_{\alpha\beta}$ , and  $C_\alpha$  are given in [12].

Assuming that the plate is loaded with transverse distributed loading  $q(\mathbf{x}, t)$  and that each lamina has homogeneous density in thickness direction, then equations of motion for Reissner linear theory for thick plates may be written as

$$M_{\alpha\beta,\beta}(\mathbf{x}, t) - Q_\alpha(\mathbf{x}, t) = I_M \ddot{w}_\alpha(\mathbf{x}, t) , \tag{8}$$

$$Q_{\alpha,\alpha}(\mathbf{x}, t) + q(\mathbf{x}, t) = I_Q \ddot{w}_\alpha(\mathbf{x}, t) , \tag{9}$$

where

$$\begin{aligned} I_M &= \int_{-h/2}^{h/2} z^2 \varrho(z) dz = \sum_{k=1}^N \int_{z_k}^{z_{k+1}} \varrho^{(k)} z^2 dz = \sum_{k=1}^N \varrho^{(k)} \frac{1}{3} (z_{k+1}^3 - z_k^3) , \\ I_Q &= \int_{-h/2}^{h/2} \varrho(z) dz = \sum_{k=1}^N \int_{z_k}^{z_{k+1}} \varrho^{(k)} dz = \sum_{k=1}^N \varrho^{(k)} (z_{k+1} - z_k) \end{aligned}$$

are global inertial characteristics of the laminate plate. If the mass density is constant throughout the plate thickness, we obtain  $I_M = \varrho h^3/12$ ,  $I_Q = \varrho h$ . Throughout the analysis, Greek indices vary from 1 to 2, and the dots over a quantity indicate differentiations with respect to time  $t$ .

#### 4. Numerical implementation of MLPG for composite plate

In MLPG method the local weak form is assembled on local subdomain  $\Omega_Q$ , which is a small domain around each node within the global domain [2]. These local subdomains overlap each other and cover the whole global domain  $\Omega$ , Fig. 3.

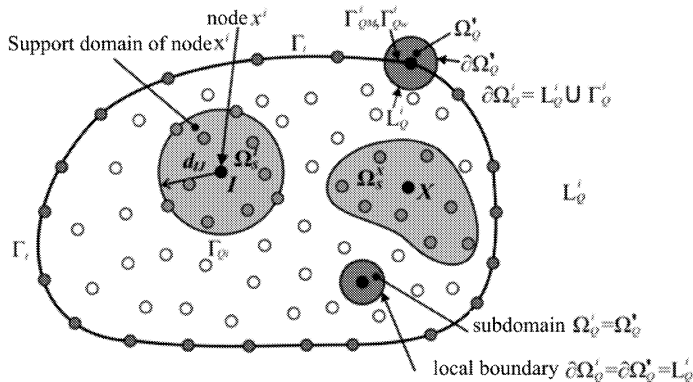


Fig.3: Local boundaries for the weak formulation, the support domain  $\Omega_s$  for MLS approximation of the trial function, and support domain of the weight function around node  $x_i$ ,  $\Omega_Q$  is the integration domain around given node

Applying the Gauss divergence theorem to the local weak form of the governing equations one obtains

$$\int_{\partial\Omega_Q^i} M_\alpha(\mathbf{x}, t) w_{\alpha\gamma}^*(\mathbf{x}) d\Gamma - \int_{\Omega_Q^i} M_{\alpha\beta}(\mathbf{x}, t) w_{\alpha\gamma,\beta}^*(\mathbf{x}) d\Omega - \int_{\Omega_Q^i} Q_\alpha(\mathbf{x}, t) w_{\alpha\gamma}^*(\mathbf{x}) d\Omega = 0, \quad (10)$$

$$\int_{\partial\Omega_Q^i} Q_\alpha(\mathbf{x}) n_\alpha(\mathbf{x}) w^*(\mathbf{x}) d\Gamma - \int_{\Omega_Q^i} Q_\alpha(\mathbf{x}) w_{,\alpha}^*(\mathbf{x}) d\Omega + \int_{\Omega_Q^i} q(\mathbf{x}) w^*(\mathbf{x}) d\Omega = 0, \quad (11)$$

where  $\partial\Omega_Q^i$  is boundary of a local subdomain,  $M_\alpha(\mathbf{x}) = M_{\alpha\beta}(\mathbf{x}) n_\beta(\mathbf{x})$  is the normal bending moment and  $n_\alpha$  is the unit outward normal on the boundary  $\partial\Omega_Q^i$ . The local weak forms (10) and (11) are starting points for deriving local boundary integral equations on the basis of proper test function. Unit step function is chosen in each subdomain as test functions  $w_{\alpha\gamma}^*(\mathbf{x})$  and  $w^*(\mathbf{x})$

$$w_{\alpha\gamma}^*(\mathbf{x}) = \begin{cases} \delta_{\alpha\gamma} & \text{for } \mathbf{x} \in (\Omega \cup \partial\Omega_s), \\ 0 & \text{for } \mathbf{x} \notin (\Omega \cup \partial\Omega_s), \end{cases} \quad w^*(\mathbf{x}) = \begin{cases} 1 & \text{for } \mathbf{x} \in (\Omega \cup \partial\Omega_s), \\ 0 & \text{for } \mathbf{x} \notin (\Omega \cup \partial\Omega_s). \end{cases} \quad (12)$$

Then the local weak form (10) and (11) transforms on the following local integral equations

$$\int_{\partial\Omega_Q^i} M_\alpha(\mathbf{x}, t) d\Gamma - \int_{\Omega_Q^i} Q_\alpha(\mathbf{x}, t) d\Omega = \int_{\Omega_Q^i} I_M \ddot{w}_\alpha(\mathbf{x}, t) d\Omega, \quad (13)$$

$$\int_{\partial\Omega_Q^i} Q_\alpha(\mathbf{x}, t) n_\alpha(\mathbf{x}) d\Gamma + \int_{\Omega_Q^i} q(\mathbf{x}) d\Omega = \int_{\Omega_Q^i} I_Q \ddot{w}_3(\mathbf{x}, t) d\Omega. \quad (14)$$

In the above local integral equations  $w_\alpha(\mathbf{x}, t)$  is the trial function corresponding to rotations,  $\alpha = 1, 2$ , the trial function  $w_3(x)$  corresponds to the transverse displacement. These trial functions are assembled in MLS approximation over nodes in local subdomain around the point  $x$ .

In general, a meshless method uses a local interpolation to represent the trial function with values (or fictitious values) of the unknown variable at some randomly located nodes [2]. To approximate a distribution of the generalized displacements (rotations and deflection) in  $\Omega_x$  over a number of randomly located nodes  $\mathbf{x}^a$ ,  $a = 1, 2, \dots, n$ , the MLS approximant  $w_i^h(\mathbf{x}, t)$  of  $w_i(\mathbf{x}, t)$  is defined by

$$\mathbf{w}^h(\mathbf{x}, t) = \sum_{a=1}^n \phi^a(\mathbf{x}) \hat{\mathbf{w}}^a(t), \quad (15)$$

where  $\mathbf{w}^h = [w_1^h, w_2^h, w_3^h]^T$ ,  $\phi^a$  is the shape function of MLS approximation corresponding to node  $\mathbf{x}^a$ . The directional derivatives of  $\mathbf{w}(\mathbf{x}, t)$  are approximated in terms of the same nodal values

$$\mathbf{w}_{,k}(\mathbf{x}, t) = \sum_{a=1}^n \hat{\mathbf{w}}^a(t) \phi_{,k}^a(\mathbf{x}), \quad (16)$$

where  $\phi_{,k}^a(\mathbf{x})$  is partial derivative of the shape function  $\phi^a(\mathbf{x})$  according to direction  $k = x_1, x_2$ .

If we ignore inertial terms in (13) and (14), then substituting the approximation (16) into the definition of the bending moments (8) and then using  $M_\alpha(\mathbf{x}) = M_{\alpha\beta}(\mathbf{x}) n_\beta(\mathbf{x})$ , one obtains

$$\mathbf{M}(\mathbf{x}) = \mathbf{N}_1 \sum_{a=1}^N \mathbf{B}_1^a(\mathbf{x}) \mathbf{w}^{*a} + \mathbf{N}_2 \sum_{a=1}^N \mathbf{B}_2^a(\mathbf{x}) \mathbf{w}^{*a} = \mathbf{N}_\alpha(\mathbf{x}) \sum_{a=1}^N \mathbf{B}_\alpha^a(\mathbf{x}) \mathbf{w}^{*a}, \quad (17)$$

where vector  $\mathbf{w}^{*a} = [\hat{w}_1^{*a}, \hat{w}_2^{*a}]^T$ , the matrices  $\mathbf{N}_\alpha(\mathbf{x})$  are related to the normal vector  $\mathbf{n}(\mathbf{x})$  and the matrices  $\mathbf{B}_\alpha^a$  are represented by the gradients of the shape functions [1].

The influence of the material properties for composite laminates is incorporated into  $C_{\alpha\beta}$  and  $D_{\alpha\beta}$ , given in [12]. Similarly, one can obtain the approximation for the shear forces

$$\mathbf{Q}(\mathbf{x}) = \mathbf{C}(\mathbf{x}) \sum_{a=1}^N [\phi^a(\mathbf{x}) \mathbf{w}^{*a} + \mathbf{F}^a(\mathbf{x}) \hat{w}_3^{*a}], \quad (18)$$

where  $\mathbf{Q}(\mathbf{x}) = [Q_1(\mathbf{x}), Q_2(\mathbf{x})]^T$  and

$$\mathbf{C}(\mathbf{x}) = \begin{bmatrix} C_1(\mathbf{x}) & 0 \\ 0 & C_2(\mathbf{x}) \end{bmatrix}, \quad \mathbf{F}^a(\mathbf{x}) = \begin{bmatrix} \phi_{,1}^a \\ \phi_{,2}^a \end{bmatrix}. \quad (19)$$

For the source point  $\mathbf{x}^i$  located on the global boundary  $\Gamma$  the boundary of the subdomain  $\partial\Omega_Q^i$  is decomposed into  $L_Q^i$  and  $\Gamma_{QM}^i$  (part of the global boundary with prescribed bending moments), Fig. 3. It should be noted here that there are neither Lagrange multipliers nor penalty parameters introduced into the local weak-forms  $\Gamma_{QM}^i$ . Part of the global boundary with prescribed rotations or displacements can be imposed directly, using the MLS approximation (15)

$$\sum_{a=1}^N \phi^a(\mathbf{x}^i) \hat{\mathbf{w}}^a = \tilde{\mathbf{w}}(\mathbf{x}^i) \quad \text{for } (\mathbf{x}^i) \in \Gamma_{QM}^i, \quad (20)$$

where  $\tilde{\mathbf{w}}(\mathbf{x}^i)$  is the generalized displacement vector prescribed on the boundary  $\Gamma_{QM}^i$ . Then, insertion of the MLS discretized moment and force fields into the local integral equations (13) and (14) we get the discretized local integral equations in the form of

$$\sum_{a=1}^n \left[ \int_{L_Q^i + \Gamma_{QM}^i} \mathbf{N}_\alpha(\mathbf{x}) \mathbf{B}_\alpha^a(\mathbf{x}) d\Gamma - \int_{\Omega_Q^i} \mathbf{C}(\mathbf{x}) \phi^a(\mathbf{x}) d\Omega \right] \mathbf{w}^{*a} - \sum_{a=1}^n \hat{w}_3^a \left[ \int_{\Omega_Q^i} \mathbf{C}(\mathbf{x}) \mathbf{F}^a(\mathbf{x}) d\Omega \right] = - \int_{\Gamma_{QM}^i} \tilde{\mathbf{M}}(\mathbf{x}) d\Gamma, \quad (21)$$

$$\sum_{a=1}^n \left[ \int_{\partial\Omega_Q^i} \mathbf{C}_n(\mathbf{x}) \phi^a(\mathbf{x}) d\Gamma \right] \mathbf{w}^{*a} - \sum_{a=1}^n \hat{w}_3^a \left[ \int_{\Omega_Q^i} \mathbf{C}_n(\mathbf{x}) \mathbf{F}^a(\mathbf{x}) d\Gamma \right] = - \int_{\Omega_Q^i} q(\mathbf{x}) d\Gamma, \quad (22)$$

Collecting the discretized local boundary-domain integral equations together with the discretized boundary conditions for the generalized displacements, one obtains a complete system of algebraic equations for calculation of strain, stress and displacement fields.

## 5. Numerical example

In this section, numerical results are presented for laminated plates under a mechanical load. Data obtained from homogenization in Part 2 are used in own MLPG software. In order to test the accuracy, numerical results obtained by the presented method are compared with the results provided by the FEM software ANSYS and ABAQUS.

The averaged percentage error (APE) was calculated by the following equation

$$APE = 100 \sqrt{\frac{\sum_{a=1}^N (u^{\text{ref}}(\mathbf{x}^a) - u^{\text{MLPG}}(\mathbf{x}^a))^2}{\sum_{a=1}^N (u^{\text{ref}}(\mathbf{x}^a))^2}}, \quad (23)$$

where  $N$  is total number of nodes in given domain,  $u^{\text{ref}}(\mathbf{x}^a)$  is the reference value in node  $\mathbf{x}^a$ ,  $u^{\text{MLPG}}(\mathbf{x}^a)$  is value calculated by means of MLPG in node  $\mathbf{x}^a$ .

Clamped and simply supported rectangular plates were analysed. We considered composite plates with dimensions  $L_x = 0.24$  m and  $L_y = 0.2$  m. Plates composed from six laminae with thickness of  $\Delta_z = 0.00025$  m, so the total thickness of plate is  $h = 0.0015$  m. Material of the analyzed plate is EGlass\_vf06. The comparison of results is given in Table 4 and Table 5. APE in the point of maximum deflection is  $|\text{err}_{\varepsilon_{11}}| = 2.3\%$  and  $|\text{err}_{\varepsilon_{22}}| = 2.95\%$ . For stress the maximum APE is  $|\text{err}_{\sigma_{11}}| = 2.58\%$  and  $|\text{err}_{\sigma_{22}}| = 2.94\%$ .

layer	1	2	3	4	5	6
$\varepsilon_{11}^{\text{MLPG}} [-]$	4.85e-04	2.90e-04	0.97e-04	-0.97e-04	-2.90e-04	-4.85e-04
$\varepsilon_{11}^{\text{ref}} [-]$	4.74e-04	2.84e-04	0.95e-04	-0.95e-04	-2.84e-04	-4.74e-04
$ \text{err}_{\varepsilon_{11}}  [\%]$	2.3	2.3	2.3	2.3	2.3	2.3
$\varepsilon_{22}^{\text{MLPG}} [-]$	9.10e-04	5.46e-04	1.82e-04	-1.82e-04	-5.46e-04	-9.10e-04
$\varepsilon_{22}^{\text{ref}} [-]$	8.84e-04	5.31e-04	1.77e-04	-1.77e-04	-5.31e-04	-8.84e-04
$ \text{err}_{\varepsilon_{22}}  [\%]$	2.95	2.95	2.95	2.95	2.95	2.95

Tab.4: Comparison of deformations  $\varepsilon_{11}$  and  $\varepsilon_{22}$  from MLPG and FEM, EGlass\_vf06

layer	1	2	3	4	5	6
$\sigma_{11}^{\text{MLPG}} [-]$	7.76e+06	3.14e+06	3.43e+06	-3.43e+06	-3.14e+06	-7.76e+06
$\sigma_{11}^{\text{ref}} [-]$	7.57e+06	3.07e+06	3.35e+06	-3.35e+06	-3.07e+06	-7.57e+06
$ \text{err}_{\sigma_{11}}  [\%]$	2.58	2.52	2.37	2.37	2.52	2.58
$\sigma_{22}^{\text{MLPG}} [-]$	10.20e+06	17.91e+06	1.50e+06	-1.50e+06	-17.91e+06	-10.20e+06
$\sigma_{22}^{\text{ref}} [-]$	9.92e+06	17.4e+06	1.46e+06	-1.46e+06	-17.4e+06	-9.92e+06
$ \text{err}_{\sigma_{22}}  [\%]$	2.85	2.94	2.88	2.88	2.94	2.85

Tab.5: Comparison of stresses  $\sigma_{11}$  and  $\sigma_{22}$  from MLPG and FEM, Eglass\_vf06

## 6. Conclusions

The MLPG method was applied to analysis of laminated composite plates under static loadings. The numerical results confirm the fact that MLPG method is a good tool for analyzing the composite structures. It is a reliable method after sufficient setting of parameters

such as order of numerical integration, size of the integration domain, support domain for weight function, etc.

Errors in strain and stress evaluation can have several sources. Accuracy of the meshless methods is affected by several factors such as rounding errors in approximation or rounding errors caused by the numerical integration. The above mentioned errors become evident in differences between the reference and computed values. FEM software compute strain or stress values at the middle surface of the layer as the arithmetic mean of strain or stress values from top and bottom surface of the layer.

### Acknowledgement

The authors gratefully acknowledge for support the Slovak and Technology Assistance Agency registered under number APVV-0736-12, Slovak Grant Agency VEGA 1/1226/12.

### References

- [1] Sládek J., Sládek V., Atluri S.N.: Application of the local boundary integral equation method to boundary-value problems, *Int. Appl. Mech.*, 38 (9), 2002, p. 1025–1047
- [2] Atluri S.N.: *The Meshless Method, (MLPG) For Domain & BIE Discretizations*, Tech Science Press, (2004)
- [3] Soares D. Jr., Sladek J., Sladek V., Zmindak M., Medvecký S: Porous Media Analysis by Modified MLPG Formulations, *CMC: Computers, Materials & Continua*, Vol. 27 (2), 2012, p. 101–127
- [4] Sladek J., Sladek V., Hellmich Ch., Eberhardsteiner J.: Analysis of thick functionally graded plates by local integral equation method, *Communications in Numerical Method in Engineering*, Vol. 23, 2007, p. 733–754
- [5] Sladek J., Sladek V., Sölk P., Wen P.H., Atluri S.N.: Thermal Analysis of Reissner-Mindlin Shallow Shells with FGM Properties by the MLPG, *CMES: Computer Modeling in Engineering & Sciences*, Vol. 30, (2), 2008, p. 77–97
- [6] Pospíšil T.: Generating non-periodic microstructures of fiber composites, *Engineering Mechanics*, Vol. 17, 2010, No. 5/6, p. 393–405
- [7] Eshelby J.D.: The determination of elastic field of an ellipsoidal inclusion and related problems, In: *Proc. R. Soc. London*, (1957), p. 276–396
- [8] Hashin Z., Shtrikman S.: On some variational principles in anisotropic and nonhomogeneous elasticity, *J. Mech. Phys. Solids*, vol. 10, 1962, p. 335–342
- [9] Kouznetsova V.G.: *Computational homogenization for the multi-scale analysis of multi-phase materials*, TU Eindhoven, 2012
- [10] Barbero E.J.: *Finite Element Analysis of Composite Materials*, CRC Press, Boca Raton, (2007)
- [11] Kormaníková E., Riecky D., Žmindák M.: Strength of Composites with Short Fibers, In: Eds, J. Murín: *Computational Modelling and Advanced Simulations*, Series: *Computational Methods in Applied Sciences*, Vol. 24, 2011
- [12] Reddy J.N.: *Mechanics of Laminated Composite Plates: Theory and Analysis*, CRC Press, Boca Raton, 1997

*Received in editor's office:* August 6, 2013

*Approved for publishing:* March 7, 2014